JOURNAL OF CATALYSIS 148, 759–770 (1994)

Self-Condensation of *n*-Butyraldehyde over Solid Base Catalysts

Hideto Tsuji, Fuyuki Yagi, Hideshi Hattori,[1] and Hideaki Kita

Division of Materials Science, Graduate School of Environmental Earth Science, Hokkaido University, Sapporo 060, Japan

Received November 22, 1993; revised March 16, 1994

The catalytic properties of various solid bases for self-condensation of *n*-butyraldehyde in liquid phase were studied to elucidate the factors governing the activity and selectivity. For alkaline earth oxide catalysts and γ-alumina catalyst, aldol condensation occurred, followed by Tishchenko-type cross-esterification of *n*-butyraldehyde with the dimer produced by the aldol condensation to form trimeric glycol ester. Alkali ion-modified alumina catalysts exhibited a high selectivity for the aldol condensation dimer, the trimeric glycol ester being formed little. Both basic and acidic sites on the surfaces of the alkaline earth oxides and γ-alumina were assumed to contribute to Tishchenko-type cross-esterification. The suppression of Tishchenko-type cross-esterification for alkali ion-modified alumina catalysts is due to the absence of acidic sites on the surfaces. The catalytic performances of alumina-supported magnesium oxide and alkali zeolite X were also examined. Alumina-supported magnesium oxide exhibited lower activity but higher selectivity to trimeric glycol ester than MgO. This catalytic feature was caused by the lower basicity and higher acidity on the surface of alumina-supported magnesium oxide as compared with MgO. The activity of alkali ion-exchanged zeolites was lowest among the catalysts examined in this study. The modification of zeolites with excess alkali ions improved the activity. © 1994 Academic Press, Inc.

INTRODUCTION

In contrast to extensive studies of solid acid catalysts, little attention has given to the studies of solid base catalysts. Solid base catalysts have been applied to a limited number of base-catalyzed reactions, although many base-catalyzed reactions are known in a homogeneous system. Recently, it has been revealed that not only single component metal oxides but also alkali modified oxides, alkali ion exchanged zeolites, and nonoxide catalysts exhibit basic properties on the surfaces (1). In addition to being an application of solid base to each base-catalyzed reaction, the elucidation of functions of catalysts for each reaction becomes more important to the design of advanced catalysts.

Aldol condensations of ketone and aldehyde are typical base-catalyzed reactions and important reactions in the petrochemical industry. In addition, the condensation reaction forming a carbon–carbon bond is useful in the synthesis of fine chemicals. Self- and cross aldol condensations of ketones and aldehydes have been studied over solid base catalysts (2–13). For aldol condensation of acetone, it was reported (11–13) that the metal oxide catalysts which have strongly basic property are effective, and that the modification of basic sites by addition of alkali metals or metal cations improves the activity. It was also suggested that the rate determining step is the formation of a new C–C bond between two acetone molecules, and that the OH groups on the alkaline earth oxide surface act as the active sites (11).

For aldol condensation of *n*-butyraldehyde in vapor phase, the studies on reduced Sn/SiO_2 catalyst (14), Ta_2O_3/SiO_2 (15), Nb_2O_3/SiO_2 (15), WO_3/SiO_2 (15), Fe_2O_3 (16), Cr_2O_3 (16), and Al_2O_3 (16) were reported, although these catalysts are not regarded as solid base catalysts. The main product over these catalysts was 2-ethyl-2-hexenal produced by dehydration of the aldol condensation dimer(2-ethyl-3-hydroxyhexanal).

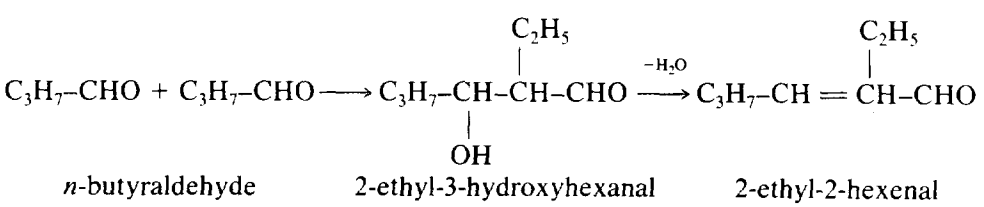

[1] To whom correspondence should be addressed.

0021-9517/94 $6.00
Copyright © 1994 by Academic Press, Inc.
All rights of reproduction in any form reserved.

Reichle reported (9) that the solid base catalyst prepared from hydrotalcite as a precursor showed the activity for aldol condensation of *n*-butyraldehyde in a vapor phase pulse reactor. The main product was 2-ethyl-2-hexenal, but the selectivities to other products were not sufficiently mentioned. In our previous paper (17), it was reported that alkaline earth oxide catalysts produced trimeric condensed product in addition to the dimeric product resulting from aldol condensation in a liquid phase. The order of activity for the aldol condensation per unit surface area was BaO > SrO > CaO > MgO, which was in accordance with the basicity of the catalysts. It was suggested that the rate determining step for aldol condensation of *n*-butyraldehyde is α-hydrogen abstraction and that the active site is the surface O^{2-}. The rate determining step and the active site for aldol condensation of *n*-butyraldehyde are different from those for aldol condensation of acetone. These differences were considered to be due to the differences in acidity of α-hydrogen between *n*-butyraldehyde and acetone.

In the present study, we wish to report the activity and selectivity for self-condensation of *n*-butyraldehyde in a liquid phase over various solid base catalysts such as alkali-modified alumina catalysts, alkali ion-exchanged zeolites, and alkaline earth oxide catalysts. We reveal that the trimeric glycol ester is formed by Tishchenko-type cross-esterification of *n*-butyraldehyde with the dimer produced by self-aldol condensation of *n*-butyraldehyde using MgO, CaO, and γ-Al_2O_3 as catalysts. On the other hand, alkali ion-modified alumina catalysts exhibited a high selectivity for aldol condensation dimer, the formation of the trimeric glycol ester being quite small. The factors governing the selectivities for the dimer and trimer are discussed from the viewpoint of acid–base properties of the catalysts.

EXPERIMENTAL METHODS

Materials

Magnesium oxide was prepared from commercial MgO (Merck) as follows. The commercial MgO powder was added to distilled water and stirred at room temperature for 24 h, then dried in an oven at 373 K to form magnesium hydroxide. Starting material for CaO was $Ca(OH)_2$(Kanto chemicals). Calcium hydroxide was also treated in distilled water in the same way as MgO. Magnesium oxide and calcium oxide were prepared by *in situ* decomposition of these hydroxides in a vacuum at elevated temperatures before use for the reaction. The alumina (γ-Al_2O_3, JRC-ALO4) used for the catalyst and the support were supplied by the Catalysis Society of Japan, which was prepared by calcining boemite powders at 973 K. This alumina contains sodium impurities of 0.01 wt% as Na_2O.

The alkali ion-modified alumina catalysts were prepared by wetness impregnation of γ-Al_2O_3 with aqueous solution of alkali acetates. The samples were dried at 373 K for 12 h, followed by calcination at 773 K for 5 h in air. The alumina catalysts modified with Na, K, and Rb ions were prepared. The contents of alkali ions were 1.2 mmol $\cdot$ g^{-1}.

Alkali ion-exchanged zeolites X and alkali ion-added zeolites X (18, 19) were prepared. Alkali ion-exchanged zeolites X were prepared by ion exchange of Linde 13X with alkali acetates followed by washing with distilled water. Alkali ion-added zeolites X were prepared by the same procedures as those used for alkali ion-exchanged zeolite except that the procedure of washing with distilled water was omitted (19). The resulting zeolites were calcined in O_2 at 673 K. The amounts of alkalis included in the alkali ion-exchanged and ion-added zeolites were determined by X-ray fluorescence analysis.

Two types of binary oxide catalysts containing magnesium and aluminum were prepared. One is alumina-supported magnesium oxide and the other is prepared by thermal decomposition of hydrotalcite. The alumina-supported magnesium oxide catalyst was prepared by impregnation of γ-Al_2O_3 with an aqueous solution of magnesium nitrate followed by drying at 373 K for 12 h and calcining at 773 K for 5 h in air. The loading amount of MgO was 3.6 mmol $\cdot$ g^{-1}. Magnesium aluminum hydroxycarbonate (hydrotalcite) with a 2 : 1 Mg : Al atomic ratio was prepared from magnesium sulfate and aluminum sulfate by coprecipitation in an aqueous solution of sodium carbonate and hydroxide (20).

Reaction Procedures

Reaction was carried out in an H-shaped glass batch reactor. The two branches were separated by a breakable seal. The fine powdered catalyst was placed in one branch, outgassed in a vacuum (ca. 1×10^{-3} Pa) at an elevated temperature for 2 h, and sealed. The known amount of *n*-butyraldehyde (Wako Pure Chemical) purified by passage through 3A molecular sieves was stored in the other branch until it was introduced through the breakable seal by distillation into the branch containing the catalyst thermostated at liquid nitrogen temperature. Reaction was started by rapid melting of the reactant at the reaction temperature followed by stirring at 600 rpm. After certain reaction time, the products were separated from the catalyst by filtering and then analyzed by GC with DEGS column. The formation of the trimer was confirmed by field desorption mass spectrometry. We referred to the products for self-condensation of *n*-butyraldehyde by using magnesium ethoxide as a catalyst in the homogeneous system (21) and identified the trimer by GC-MASS.

Temperature-Programmed Desorption Analysis

To examine the amount and strength of basic sites on the surface of catalysts, temperature-programmed de-

sorption (TPD) analysis for the adsorbed carbon dioxide was carried out. A catalyst (0.05 g) evacuated at a certain pretreatment temperature for 2 h was exposed to 1.3 kPa of CO_2 at room temperature for 10 min followed by evacuation at room temperature for 30 min. The TPD was run at a heating rate of 10 $K \cdot min^{-1}$ from room temperature to 773 K. The desorbed gases were analyzed by mass spectrometry. A quadrupole mass spectrometer (ANELVA AQA100R) was used. Peak intensities of the desorbed gases were normalized to that of Ar which was constantly introduced into the system as an internal standard. For examination of the acid sites, TPD analysis of the adsorbed NH_3 was done in the same procedure.

RESULTS

Surface Area, Chemical Composition, and XRD Analysis of the Catalysts

The specific surface areas determined by nitrogen adsorption at liquid nitrogen temperature and the chemical compositions of the catalysts are given in Table 1. It is well known that the surface area of alkaline earth oxide varies with the pretreatment temperature. The surface areas of MgO and CaO prepared by *in situ* decomposition of the hydroxides in a vacuum at 873 K were 172 $m_2 \cdot g^{-1}$ and 68 $m^2 \cdot g^{-1}$, respectively.

The specific surface areas of alkali ion-modified alumina catalysts were practically the same as that of γ-Al_2O_3. In the XRD patterns of alkali ion-modified alumina, only the γ-Al_2O_3 phase was appreciable. This suggests that the alkali ion doping does not provoke any considerable changes in the γ-Al_2O_3 texture.

For the alumina-supported magnesium oxide catalyst, the specific surface area was practically the same as that of γ-Al_2O_3. This also indicates that the magnesium ion doping does not provoke any considerable changes in the γ-Al_2O_3 texture. In addition to the XRD pattern of γ-Al_2O_3, the XRD pattern of MgO(200) appeared, although the peaks were broad as compared with those of bulk MgO.

Magnesia–alumina catalysts prepared by decomposition of hydrotalcite at 773 K possess a surface area of 251 $m^2 \cdot g^{-1}$. Thermal treatment above 673 K decomposed hydrotalcite to magnesia–alumina. The fine particles of MgO were observed in XRD pattern for the sample pretreated above 673 K. The calculated content of MgO was 15.3 $mmol \cdot g^{-1}$ for the resulting MgO–Al_2O_3.

The amounts of alkalis in the alkali ion-added zeolites were larger than those of the alkali ion-exchanged zeolites for all kinds of alkalis. The excess alkalis are supposed to locate in the cavities of zeolites in the form of oxide. Judging from the specific surface areas, the crystallinities

TABLE 1

Surface Area and Chemical Composition of the Catalysts

Catalysts	Surface area($m^2 \cdot g^{-1}$)	% Exchange	Loading amounts ($mmol \cdot g^{-1}$)	XRD pattern
MgO[a]	172[d,g]	—	—	MgO[j]
CaO[b]	68[d,g]	—	—	CaO[j]
γ-Al_2O_3	172[e,g]	—	—	γ-Al_2O_3
Na/Al_2O_3	163[e,g]	—	1.2	γ-Al_2O_3
K/Al_2O_3	147[e,g]	—	1.2	γ-Al_2O_3
Rb/Al_2O_3	132[e,g]	—	1.2	γ-Al_2O_3
Mg/Al_2O_3	150[f,g]	—	3.6	MgO + γ-Al_2O_3
MgO–Al_2O_3[c]	251[e,g]	—	15.3[i]	MgO[j]
NaX(13X)	780[f,h]	100	—	—
KX	690[f,h]	99	—	—
RbX	550[f,h]	76	—	—
Na/NaX	760[f,h]	110	0.40	—
K/KX	660[f,h]	112	0.59	—
Rb/RbX	420[f,h]	81	0.27	—

[a] Prepared by *in situ* decomposition of $Mg(OH)_2$.
[b] Prepared by *in situ* decomposition of $Ca(OH)_2$.
[c] Prepared by *in situ* decomposition of hydrotalcite(Mg : Al = 2 : 1).
[d] Pretreatment temperature = 873 K.
[e] Pretreatment temperature = 773 K.
[f] Pretreatment temperature = 673 K.
[g] Calculated by application of BET isotherm to nitrogen adsorption at 77 K.
[h] Calculated by application of Langmuir isotherm to nitrogen adsorption at 77 K.
[i] Mg content of gram MgO–Al_2O_3 prepared from hydrotalcite(Mg : Al = 2 : 1).
[j] XRD measurement was performed after thermal pretreatment.

of the zeolites are retained during ion exchange and oxide formation processes.

Activity and Selectivity for Self-Condensation of n-Butyraldehyde over Magnesium Oxide, Calcium Oxide, and Alumina Catalysts

The activities and selectivities of MgO and CaO are given in Table 2. The selectivity for each product was expressed by the mol% of *n*-butyraldehyde converted to each product in the total *n*-butyraldehyde converted. The main products were 2-ethyl-3-hydroxyhexanal (ACD) produced by aldol condensation, and 2-ethyl-2-hexenal (2EHA) produced by dehydration of 2-ethyl-3-hydroxyhexanal, and the trimer(TGE), which is glycol ester(I) formed by Tishchenko-type cross-esterification of *n*-butyraldehyde with the dimer produced by aldol condensation of *n*-butyraldehyde. The mole ratio of *n*-butyraldehyde converted to the aldol condensation dimer to the trimeric glycol ester was taken as the ratio of the dimer to the trimer, and is listed as ACD/TGE in Table 2. In addition to these products, small amounts of *n*-butyl-*n*-butyrate(II) and butanol, which are tabulated as others, were formed for all catalysts listed in Table 2.

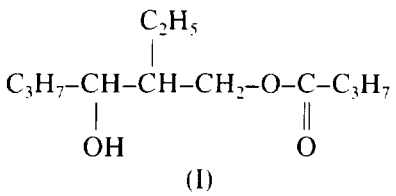

(I)

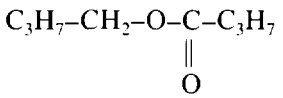

(II)

Calcium oxide was slightly more active than MgO, and the conversion to the trimeric glycol ester was much higher for CaO than for MgO at the reaction temperature of 273 K. As the reaction temperature was raised, the conversion became high and the ratio of the dimer to the trimer decreased. The selectivity to 2-ethyl-2-hexenal also increased as the reaction temperature was raised from 273 to 323 K.

γ-Alumina catalyst exhibited the activity, although the activity was lower than those of MgO and CaO. A considerable amount of trimeric glycol ester was formed. This indicates that γ-Al_2O_3 catalyzes not only aldol condensation but also Tishchenko reaction of the aldol condensation dimer with *n*-butyraldehyde. The selectivities to 2-ethyl-2-hexenal and *n*-butyl-*n*-butyrate were higher for γ-Al_2O_3 than for MgO and CaO.

The selectivities to *n*-butyl-*n*-butyrate and butanol were less than 1% for all the catalysts examined. *n*-Butyl-*n*-butyrate is considered to be formed by Tishchenko-type self-esterification of *n*-butyraldehyde. The formation of a small amount of *n*-butyl-*n*-butyrate indicates that the rate of Tishchenko-type cross-esterification of the aldol condensation dimer with *n*-butyraldehyde is faster than that of the self-esterification of *n*-butyraldehyde.

Variations of the Activity and Selectivity of MgO as a Function of Pretreatment Temperature

The variations of the activity and selectivity of MgO with the pretreatment temperature are shown in Fig. 1. Maximum total conversion appeared around the pretreatment temperature of 873 K. The ratio of the aldol condensation dimer to the trimeric glycol ester decreased monotonically as the pretreatment temperature increased. The amount of the trimeric glycol ester formed was larger for the MgO pretreated at 1273 K than for the MgO pretreated at 873 K.

TABLE 2

Activities of MgO, CaO, and γ-Al_2O_3 for Self-Condensation of *n*-Butyraldehyde

Catalyst	Catalyst weight (mg)	Reaction temp. (K)	Reaction time (h)	Conv. (%)	Selectivity[a] (%)				ACD/TGE[b]
					2EHA	ACD	TGE	Others	
MgO[c]	10	323	1[e]	52	3.1	73.9	22.6	0.3	3.3
MgO[c]	50	273	1[f]	35	1.7	81.7	16.3	0.3	5.0
CaO[c]	50	273	1[f]	41	2.8	39.8	56.9	0.5	0.7
γ-Al_32O_3[d]	50	323	2[e]	33	19.4	58.8	20.9	0.9	2.8

[a] 2EHA, 2-ethyl-2-hexenal; ACD, aldol condensation dimer (2-ethyl-3-hydroxyhexanal); TGE, trimeric glycol ester; others include *n*-butyl-*n*-butyrate and butanol.

[b] Mole ratio of *n*-butyraldehyde converted to each product.

[c] Pretreatment temperature = 873 K.

[d] Pretreatment temperature = 773 K.

[e] 7 mmol of *n*-butyraldehyde.

[f] 14 mmol of *n*-butyraldehyde.

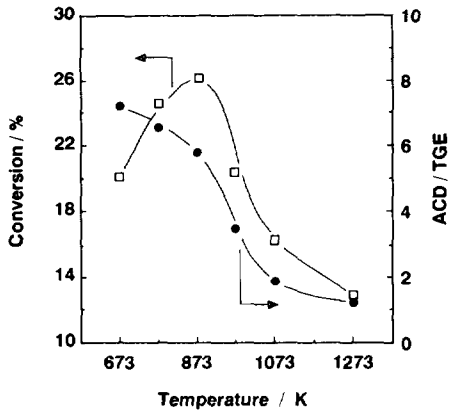

FIG. 1. Pretreatment temperature dependence of the conversion of *n*-butyraldehyde and the ratio of dimer/trimer for MgO. The ratio ACD/TGE is the ratio of *n*-butyraldehyde converted to aldol condensation dimer/trimeric glycol ester. Reaction temperature, 273 K; reaction time, 0.5 h; 50 mg of catalyst; 14 mmol of *n*-butyraldehyde.

Activity and Selectivity for Self-Condensation of n-Butyraldehyde over Alkali Ion-Modified Alumina Catalysts

The activities and selectivities of alkali ion-modified alumina catalysts are listed in Table 3. The activity for aldol condensation of γ-Al_2O_3 was extensively enhanced by the modification with alkali ion. The order of activity was $Rb/Al_2O_3 \geq K/Al_2O_3 > Na/Al_2O_3$. The activities for aldol condensation of *n*-butyraldehyde were higher for Rb/AL_2O_3 and K/Al_2O_3 than for MgO.

A great difference between the alkali ion-modified alumina catalysts and alkaline earth oxide catalysts was observed in the formation of the trimeric glycol ester. For the alkali ion-modified alumina catalysts, the formation of the trimeric glycol ester was not significant. The ratios of the aldol condensation dimer to the trimeric glycol ester were more than 30, and increased in the order $Na/Al_2O_3 < K/Al_2O_3 < Rb/Al_2O_3$. The ratio of 2-ethyl-2-hexenal to the aldol condensation dimer was low for alkali ion-modified alumina catalysts, and the formations of *n*-butyl-*n*-butyrate and butanol were scarcely observed.

Activity and Selectivity for Self-Condensation of n-Butyraldehyde over Alumina-Supported Magnesium Oxide Catalyst and Magnesia–Alumina Catalyst Prepared from Hydrotalcite

The activity and selectivity of the alumina-supported magnesium oxide catalyst (MgO content 3.6 mmol $\cdot g^{-1}$) are given in Table 4. The total conversion of MgO/Al_2O_3 was slightly higher than that of γ-Al_2O_3. The conversion to trimeric glycol ester was high, whereas the conversion to 2-ethyl-2-hexenal was low as compared with the rates for γ-Al_2O_3. The ratio of the aldol condensation dimer to the trimeric glycol ester was smaller for MgO/Al_2O_3 than for MgO. it is suggested that the ratio of the rate of Tishchenko-type cross-esterification of the aldol condensation dimer with *n*-butyraldehyde to the rate of self-aldol condensation of *n*-butyraldehyde is higher for MgO/Al_2O_3 than for MgO, although the total conversion of *n*-butyraldehyde is higher for MgO than for MgO/Al_2O_3.

The results with the magnesia–alumina catalyst prepared by *in situ* decomposition of hydrotalcite are given in Table 4. The catalyst exhibited similar behavior as alumina-supported magnesium oxide catalyst. The total conversion of *n*-butyraldehyde was almost at the same level as that of γ-Al_2O_3 and lower than that of MgO. The ratio of the rate of Tishchenko-type cross-esterification to the rate of self-aldol condensation of *n*-butyraldehyde was also higher for $MgO–Al_2O_3$ than for MgO.

Activity and Selectivity for Self-Condensation of n-Butyraldehyde over Alkali Ion-Exchanged Zeolites and Alkali Ion-Added Zeolites

The activities and selectivities of the zeolite catalysts for self-condensation of *n*-butyraldehyde are given in Ta-

TABLE 3

Activities of Alkali Ion-Modified Alumina for Self-Condensation of *n*-Butyraldehyde

Catalyst	Catalyst weight (mg)	Reaction temp. (K)	Reaction time (h)	Conv. (%)	Selectivity[a] (%)				ACD/TGE[b]
					2EHA	ACD	TGE	Others	
Na/Al_2O_3[c]	10	323	0.5[d]	28	5.4	92.0	2.6	—	35
K/Al_2O_3[c]	10	323	0.5[d]	50	3.9	93.8	2.2	—	43
Rb/Al_2O_3[c]	10	323	0.5[d]	53	3.3	95.7	1.0	—	96

[a] 2EHA, 2-ethyl-2-hexenal; ACD, aldol condensation dimer (2-ethyl-3-hydroxyhexanal); TGE, trimeric glycol ester; others include *n*-butyl-*n*-butyrate and butanol.

[b] Mole ratio of *n*-butyraldehyde converted to each product.

[c] Pretreatment temperature = 773 K.

[d] 7 mmol of *n*-butyraldehyde.

TABLE 4

Activities of Alumina-Supported Magnesium Oxide and Magnesia–Alumina for Self-Condensation of *n*-Butyraldehyde

Catalyst	Catalyst weight (mg)	Reaction temp. (K)	Reaction time (h)	Conv. (%)	Selectivity[a] (%) 2EHA	ACD	TGE	Others	ACD/TGE[b]
MgO/Al_2O_3[c]	50	323	2[e]	37	9.8	58.7	30.8	0.8	1.9
$MgO–Al_2O_3$[c]	50[d]	323	2[e]	31	11.0	60.5	28.1	0.3	2.2

[a] 2EHA, 2-ethyl-2-hexenal; ACD, aldol condensation dimer (2-ethyl-3-hydroxyhexanal); TGE, trimeric glycol ester; others include *n*-butyl-*n*-butyrate and butanol.
[b] Mole ratio of *n*-butyraldehyde converted to each product.
[c] Pretreatment temperature = 773 K.
[d] 50 mg of hydrotalcite(Mg : Al = 2 : 1) was used as catalyst precursor.
[e] 7 mmol of *n*-butyraldehyde.

ble 5. The total conversions per unit weight of alkali ion-exchanged zeolites were much lower than those of MgO, CaO, γ-Al_2O_3, and alkali ion-modified alumina. The activities of alkali ion-added zeolites were higher than those of alkali ion-exchanged zeolites but still lower than those of MgO, CaO, and alkali ion-modified alumina catalysts.

The considerable selectivity to the trimeric glycol ester was observed for both alkali ion-exchanged zeolites and alkali ion-added zeolites. The selectivity to 2-ethyl-2-hexenal was higher for the zeolite catalysts than for MgO, CaO, and alkali ion-modified alumina catalysts.

Temperature-Programmed Desorption of Carbon Dioxide and Ammonia

The TPD plots of carbon dioxide adsorbed on the catalysts are shown in Fig. 2. In TPD of the adsorbed CO_2, the concentration of the basic sites is reflected in the peak area of TPD plot, and in the strength of the basic sites in the temperature at which CO_2 desorption peak appears. Although TPD plots of adsorbed CO_2 are broad, we observe a correlation between the amount of basic sites and the activity for self-condensation of *n*-butyraldehyde. For alkali ion-exchanged zeolites and alkali ion-added zeolites, TPD plots of adsorbed CO_2 have been reported (19). Both the concentration and the strength of the basic sites are higher for alkali ion-added zeolites than for alkali ion-exchanged zeolites, but are much lower than for MgO and Rb/Al_2O_3.

The TPD plot of adsorbed CO_2 for γ-Al_2O_3 also exhibits a significant desorption peak. This indicates that γ-Al_2O_3 possesses the basic sites though they are relatively weak. For alkali ion-modified alumina catalysts, the amounts of desorbed CO_2 were larger than for γ-Al_2O_3. Furthermore, the desorption occurred at higher temperatures for alkali ion-modified alumina catalysts than for γ-Al_2O_3. The modification of the γ-Al_2O_3 surface with alkali ions increased both the amount and the strength of the basic sites. Addition of magnesium ions to γ-Al_2O_3 resulted in small increases in both the amount and strength of the basic sites.

TABLE 5

Activities of Alkali Ion-Exchanged and Ion-Added Zeolites for Self-Condensation of *n*-Butyraldehyde

Catalyst	Catalyst weight (mg)	Reaction temp. (K)	Reaction time (h)	Conv. (%)	Selectivity[a] (%) 2EHA	ACD	TGE	Others	ACD/TGE[b]
NaX(13X)[c]	50	323	5[d]	2	16.6	72.9	10.6	—	6.9
KX[c]	50	323	5[d]	2	14.2	79.2	6.5	—	12
RbX[c]	50	323	5[d]	4	6.8	86.8	6.3	—	14
Na/NaX[c]	50	323	5[d]	63	12.5	81.3	5.9	0.2	14
K/KX[c]	50	323	5[d]	62	15.9	78.7	5.1	0.2	15
Rb/RbX[c]	50	323	5[d]	53	13.3	81.8	4.6	0.2	18

[a] 2EHA, 2-ethyl-2-hexenal; ACD, aldol condensation dimer (2-ethyl-3-hydroxyhexanal); TGE, trimeric glycol ester; others include *n*-butyl-*n*-butyrate and butanol.
[b] Mole ratio of *n*-butyraldehyde converted to each product.
[c] Pretreatment temperature = 773 K.
[d] 7 mmol of *n*-butyraldehyde.

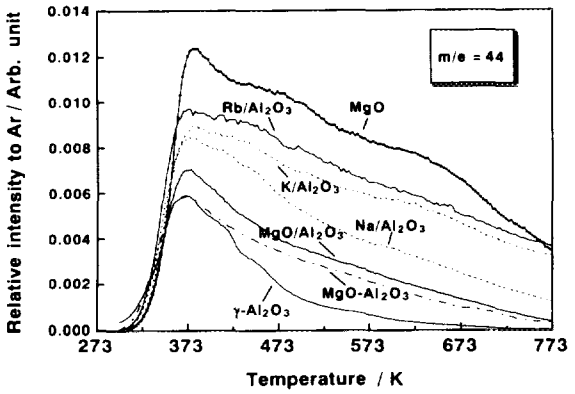

FIG. 2. TPD plots of the adsorbed CO_2. Heating rate, 10 K · min^{-1}; 50 mg of sample. Pretreatment temperature of catalyst: 873 K for MgO, 773 K for others.

It is indicated that the modification with alkali ions is more effective for the increase of both the amount and the strength of the basic sites than the modification with magnesium ions. The order of basicity estimated by TPD plots of adsorbed CO_2 is as follows: MgO > alkali ion-modified alumina > $MgO/Al_2O_3 \approx MgO-Al_2O_3 > \gamma$-$Al_2O_3$. The order of basicity, except the order of MgO and K and Rb ion-modified aluminas, is in accordance with the order of the total conversion for self-condensation of *n*-butyraldehyde.

The TPD plots of adsorbed NH_3 are shown in Fig. 3. Magnesium oxide also exhibited significant NH_3 desorption, although the amount of the desorbed NH_3 was smaller than that for γ-Al_2O_3. It was reported that ammonia is adsorbed on MgO and undergoes heterolytic dissociation on Mg^{2+}–O^{2-} *ion-pair* sites (22, 23). The Mg^{2+} sites act as acidic sites and adsorb NH_2^-. The TPD plot of the adsorbed NH_3 on CaO suggests that CaO also possesses such acidic sites on the surface.

While the acidic sites exist on γ-Al_2O_3 surface, the desorption of NH_3 was not significant for Rb/Al_2O_3. This

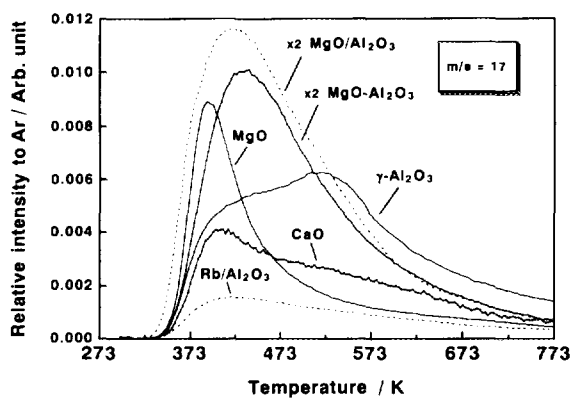

FIG. 3. TPD plots of the adsorbed NH_3. Heating rate, 10 K · min^{-1}; 50 mg of sample. Pretreatment temperature of catalyst: 873 K for MgO and CaO, 773 K for others.

indicates that the acidic sites of γ-Al_2O_3 surface are greatly suppressed by modification with Rb^+ ions. The amounts of acidic sites on MgO/Al_3O_3 and $MgO-Al_2O_3$ were similar, and larger than those of MgO and γ-Al_2O_3.

DISCUSSION

Surface Properties Governing the Selectivity for Self-Condensation of n-Butyraldehyde

One of our findings is the formation of the trimeric glycol ester by the Tishchenko-type cross-esterification for alkaline earth oxide catalysts and γ-alumina catalyst in the liquid phase self-condensation of *n*-butyraldehyde. This reaction was strongly suppressed for the alkali ion-modified alumina catalysts, and, therefore, the products resulting from aldol condensation can be selectively obtained. In this section, we discuss the surface properties which govern the product distribution, namely the active sites for the Tishchenko-type cross-esterification.

The TPD plots of adsorbed CO_2 (Fig. 2) indicate that all catalysts which are active for aldol condensation of *n*-butyraldehyde possess basic sites on their surfaces. It is suggested that the basic sites on these surfaces are active sites for aldol condensation of *n*-butyraldehyde. Except for MgO and K and Rb ion-modified aluminas, the order of surface basicity is in agreement with the order of the conversion for aldol condensation of *n*-butyraldehyde. The reasons for the lower activity of MgO as compared to K and Rb ion-modified aluminas are unclear. The formation of the trimeric glycol ester was much larger for MgO. The blocking of the active sites with the trimeric glycol ester may retard the aldol condensation on MgO surface.

It was reported that alumina is an effective catalyst for base-catalyzed organic reactions such as aldol condensation of ketone (24, 25), Knoevenagel condensation (26), and Michael addition (27) under a mild condition. We confirmed the effectiveness of γ-Al_2O_34 for the self-condensation of *n*-butyraldehyde. The basic sites on γ-Al_2O_3 seem to be relevant to the reaction.

According to the results of TPD of adsorbed CO_2, the amount and the strength of basic sites are larger for alkali ion-modified alumina catalysts than for ion-modified γ-Al_2O_3. Tishchenko-type esterification is closely related to the Cannizzaro reaction, which is generally considered to be a base-catalyzed reaction. However, the formation of the trimeric glycol ester which is produced by the Tishchenko-type cross-esterification was completely suppressed for alkali ion-modified alumina catalysts. Therefore, the occurrence of the Tishchenko-type cross-esterification cannot be explained only by the basic property of catalysts. Indeed, the trimeric glycol ester was formed for MgO, which exhibits the basicity in the same

level as alkali ion-modified alumina catalysts as shown in TPD plots of the adsorbed CO_2 (Fig. 2).

The TPD plots of the adsorbed NH_3 (Fig. 3) indicate that γ-Al_2O_3 possesses acidic sites. Magnesium oxide also exhibited significant NH_3 desorption in the TPD plot. While the acidic sites exist on both MgO and γ-Al_2O_3 surfaces, the desorption of NH_3 was not significant for Rb/Al_2O_3. This indicates that the acidic sites of γ-Al_2O_3 surface are greatly suppressed by the modification with Rb^+ ions. We consider that such suppression of the acidic sites results in the selective formation of the dimer by aldol condensation for alkali ion-modified alumina catalysts. In other words, the acidic sites on the catalysts participate in the Tishchenko-type cross-esterification. The participation of the acidic sites in the Tishchenko-type cross-esterification is supported by the enhanced selectivity to the trimeric glycol ester for MgO/Al_2O_3 and $Mgo-Al_2O_3$, which possess a large amount of acidic sites as shown in TPD plots of the adsorbed NH_3 (Fig. 3).

It is known that dehydration of alcohols is catalyzed by acidic sites of catalysts. In the formation of 2-ethyl-2-hexenal which is formed by the dehydration of the aldol condensation dimer, the acidic sites are considered to be involved. The catalysts which promoted the Tishchenko-type cross-esterification also produced a significant amount of 2-ethyl-2-hexenal. The low ratio of 2-ethyl-2-hexenal to the aldol condensation dimer for the alkali ion-modified alumina catalysts is also due to the neutralization of the acidic sites on the γ-Al_2O_3 surface by the modification with alkali ions. The neutralization of the acidic sites is considered to be caused by an electronic effect of alkalis. The XPS study of sodium ion doped γ-Al_2O_3 showed that the surface coverage of Na^+ increase linearly with the concentration of doped Na^+ and suggested the formation of –Al–O–Na surface groups (28). The efficient suppresion of the acidic sites on γ-Al_2O_3 must result from the uniform dispersion of alkalis.

Mechanism of Tishchenko Reaction-Type Cross-Esterification

Tanabe and Saito reported that alkaline earth oxides proceed the Tishchenko reaction of benzaldehyde to form benzylbenzoate (29). They also pointed out the participation of the acidic sites on the surface for Tishchenko reaction, although the activity for the Tishchenko reaction depends on basicity of the catalysts.

There is a great difference in the reaction pathway between benzaldehyde and *n*-butyraldehyde. Benzaldehyde has no α-hydrogen, but *n*-butyraldehyde has. Therefore, benzaldehyde cannot undergo aldol condensation. In the present study, we reveal that *n*-butyraldehyde undergoes both Tishchenko reaction and aldol condensation over solid base catalysts. Tishchenko reaction competes with aldol condensation for self-condensation of *n*-butyraldehyde.

The reaction scheme for self-condensation of *n*-butyraldehyde is shown in Fig. 4. The reaction pathway for the catalysts such as MgO, CaO, and γ-Al_2O_3 is recognized as aldol condensation of *n*-butyraldehyde followed by Tishchenko-type cross-esterification of the aldol condensation dimer with *n*-butyraldehyde. However, the reaction rate of the Tishchenko-type self-esterification to *n*-butyl-*n*-butyrate is much lower than those of the aldol condensation of *n*-butyraldehyde and the Tishchenko-type cross-esterification. The reason for the slow rate of the self-esterification as compared with the cross-esterification is not clear.

A relation between the acid–base properties of catalysts and product distribution in self-condensation of *n*-butyral-

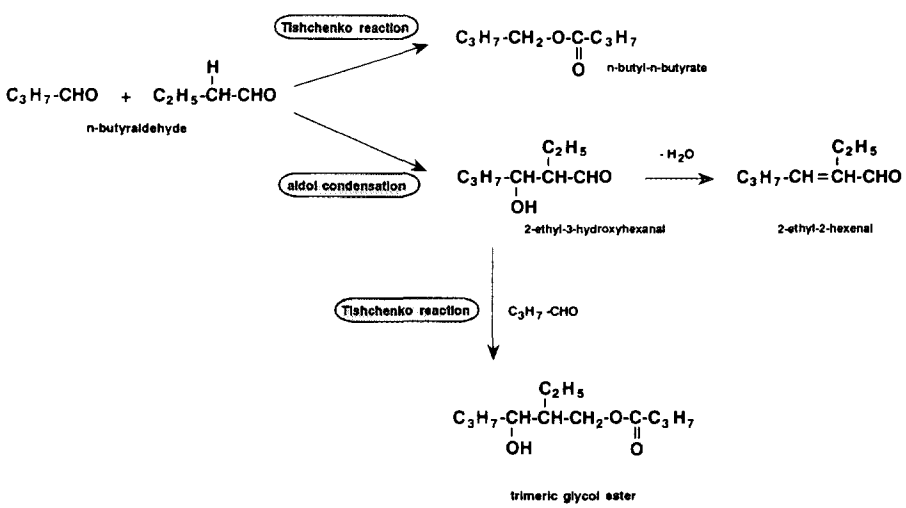

FIG. 4. Reaction scheme for self-condensation of *n*-butyraldehyde over solid base catalysts.

dehyde has been reported for metal alkoxide catalysts by Villani and Nord (21). They showed that mildly basic ethoxide catalysts such as $Mg(OC_2H_5)_2$ and $Ca(OC_2H_5)_2$ lead to the formation of the trimeric glycol ester in preference to the simple ester, while the highly basic $Na(OC_2H_5)$ produces only aldol condensation products. The acidic ethoxide, $Al(OC_2H_5)_3$, promotes the Tishchenko-type self-esterification to produce the simple ester. Villani and Nord suggested that the formation of the trimeric glycol ester is attributed to a bifunctional action of the catalysts. Namely, the aldol condensation is promoted by the basic nature of the catalysts and then the Tishchenko-type cross-esterification by the acidic nature. Villani and Nord interpreted that the predominant occurrence of the aldol condensation in the self-condensation of *n*-butyraldehyde for mildly basic alkoxide catalysts is caused by the existence of α-hydrogen in *n*-butyraldehyde. However, the existence or absence of α-hydrogen cannot explain the preferential occurrence of the Tishchenko-type cross-esterification in the successive step, because aldol condensation dimer(2-ethyl-3-hydroxyhexanal) has α-hydrogen. We consider that there must be other reasons such as steric and electronic effects resulting from the structure of the aldol condensation dimer for the preferential occurrence of the Tishchenko-type cross-esterification in the successive step.

The studies of metal alkoxide catalysts for self-condensation of aldehydes which have α-hydrogen did not point out the role of the basic nature of catalysts in Tishchenko-type self- and cross-esterification (21, 30–32). The study on the Tishchenko reaction of benzaldehyde over alkaline earth oxide catalysts showed that the activity of CaO is higher than that of MgO, and that this order is in agreement with the basicity of the catalyst surface (29). In the present study, the ratio of the aldol condensation dimer to the trimeric glycol ester is higher for CaO than for MgO and γ-Al_2O_3. As estimated byTPD plot of the adsorbed NH_3, the amount of acidic sites on the CaO surface is smaller than those on MgO and γ-Al_2O_3. Thus, it is suggested that basic sites also play a role in catalyzing the Tishchenko reaction. We believe that MgO, CaO, and γ-Al_2O_3 catalyze Tishchenko-type cross-esterification in such a bifunctional way that both basic and acidic sites are involved.

We refer to the mechanisms of the Tishchenko reaction proposed for metal alkoxide catalysts (31, 32); the mechanisms of Tishchenko-type cross-esterification over the catalysts such as MgO, CaO, and γ-Al_2O_3 are proposed as illustrated in Fig. 5. The acid site on the surface(M) interacts with the carbonyl oxygen of aldehyde to form the intermediate(II). Then, the carbonyl oxygen of the other aldehyde adsorbed on basic site(O) (intermediate(III)) reacts with the carbonyl carbon of the intermediate(II) to form the intermediate(IV). Finally, an intramolecular hydride transfer occurs to form ester. It is plausible for the basic sites to interact with the carbon of the carbonyl group (intermediate(III)) and enhance the reactivity of the carbonyl oxygen to facilitate step(ii).

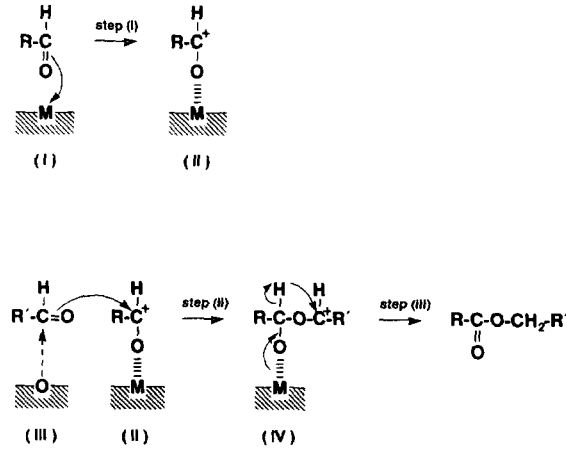

FIG. 5. The proposed mechanism for Tishchenko-type cross-esterification over alkaline earth oxides. RCHO and R'CHO represent *n*-butyraldehyde and 2-ethyl-3-hydroxyhexanal (aldol condensation dimer), respectively.

In the cross-esterification, two types of esters would have been formed if the intermediate(II) and intermediate(III) were formed equally from *n*-butyraldehyde and 2-ethyl-3-hydroxyhexanal. In the present study, however, one type ester(R− = *n* − C_3H_{7-}, R'− = $CH_3CH_2CH_2CH(OH)CH(C_2H_5)-$) was exclusively formed. Exclusive formation of the ester was also observed in metal alkoxide catalyst systems (21, 30–32). This indicates the preferential formation of the intermediates (I) and (III) from *n*-butyraldehyde and 2-ethyl-3-hydroxyhexanal, respectively. The basic sites interact much more easily with the carbonyl carbon of 2-ethyl-3-hydroxyhexanal than with that of *n*-butyraldehyde probably because of the structural and electronic properties of 2-ethyl-3-hydroxyhexanal. The preferential formation of the intermediate(III) from 2-ethyl-3-hydroxyhexanal also accounts for the higher rate of the cross-esterification as compared with the self-esterification of *n*-butyraldehyde.

Acid Sites on the Surface of Magnesium Oxide

In the present study, we confirmed the existence of the acidic sites on the surfaces of MgO and CaO, although alkaline earth oxides have been classified into strong solid base catalysts. The surface structure and chemical properties of MgO have been studied in relation to coordinatively unsaturated ion sites on the surface. On thoroughly degassed MgO surface, coordinatively unsaturated Mg^{2+} cations are exposed and exhibit Lewis-acidic nature (33). For the adsorption of ammonia (22, 23), hydrogen (34–37), and hydrocarbons (38–40) with heterolytic dissociation,

the acidic sites of coordinative unsaturated Mg^{2+} cations play an important role.

Although the surface of MgO sinters with increasing the pretreatment temperature, the lower coordinated Mg^{2+} cation sites become exposed at a higher temperature, resulting in desorption of adsorbate (41). As the coordination number of O^{2-} to Mg^{2+} decreases, LUMO level of Mg^{2+} sites becomes lower because of the decrease in Madelung potential, and the reactivity of Mg^{2+} sites is enhanced (42). Molecular orbital calculation also pointed out that the acidity of the Mg^{2+} becomes stronger as the coordination number of O^{2-} to Mg^{2+} decreases (43). The ratio of the aldol condensation dimer to the trimeric glycol ester decreased monotonically as the pretreatment temperature increased (Fig. 1). The observed tendency of the formation of trimeric glycol ester as a function of pretreatment temperature is in accordance with the manner of exposure of lower coordinated Mg^{2+} cations on the MgO surface. Therefore, it is concluded that the coordinatively unsaturated Mg^{2+} cations act as effective acidic sites for the Tishchenko-type cross-esterification.

The total conversion reached the maximum at the pretreatment temperature of 873 K, and decreased as the pretreatment temperature increased further. The decrease in the total conversion was caused by the decrease in the activity for aldol condensation of *n*-butyraldehyde. The surface area decreased to 90 $m^2 \cdot g^{-1}$ for MgO pretreated at 1273 K, whereas the area for MgO pretreated at 873 K was 172 $m^2 \cdot g^{-1}$. Thus, the decrease of the activity of MgO for aldol condensation is suggested to be due mainly to the decrease in the surface area.

Catalytic Action of Alumina-Supported Magnesium Oxide and Magnesia–Alumina Catalyst Prepared from Hydrotalcite

The alumina-supported magnesium oxide catalyst (MgO 3.6 $mmol \cdot g^{-1}$) pretreated at 773 K exhibited the characteristic feature in the sense that the trimeric glycol ester was formed in a high selectivity. The catalytic performance of the supported magnesium oxide is different from that of the bulk magnesium oxide. The difference is considered to result from the change in the acid–base property.

The TPD plots of the adsorbed NH_3 showed that the amount of acidic sites on the MgO/Al_2O_3 surface pretreated at 773 K is larger than that of MgO pretreated at 873 K. The enhanced acidity of MgO/Al_2O_3 can be regarded as one of the factors to increase the selectivity to the trimeric glycol ester. The lower basicity on MgO/Al_2O_3 surface as compared with MgO was shown by TPD analysis of the adsorbed CO_2 (Fig. 2). It is considered that the lower basicity results in the low activity of MgO/Al_2O_3 for aldol condensation, and also leads to the high selectivity for the trimeric glycol ester.

The enhancement of acidity of MgO/Al_2O_3 as compared with MgO may be simply explained by the increase in the concentration of coordinatively unsaturated Mg^{2+} cation sites which act as acidic sites. Because the particle size of MgO is small as determined by XRD, the MgO on γ-Al_2O_3 should have large numbers of coordinatively unsaturated Mg^{2+} cation sites on the surface. It is also suggested that the dispersed small particle MgO and/or the interaction with oxide support form the intrinsic surface electronic structures and generate the new acid sites (44).

The product distribution was similar for the magnesia–alumina catalyst prepared from hydrotalcite and for alumina-supported magnesium oxide. The thermal treatment of hydrotalcite results in the formation of small MgO particles incorporating Al^{3+} cations and having high surface area (20, 45, 46). The basic property of this high surface area MgO prepared from hydrotalcite has been studied by McKenzie *et al.* (46). They reported that the incorporation of aluminum into MgO suppresses the formation of strongly basic sites which are normally present on the surface of bulk MgO. In the present study, the TPD plots of adsorbed CO_2 also indicate that the amount of strongly basic sites is smaller for $MgO–Al_2O_3$ than for MgO. The decrease in the number of the strongly basic sites on the surface results in the low activity for aldol condensation and, consequently, attains the high selectivity for the trimeric glycol ester.

The suppression of the strongly basic sites on MgO surface by the incorporation of aluminum into MgO may be applicable to the case of alumina-supported magnesium oxide. Nevertheless, the recent study of the surface acid–base properties of nanoscale ultrafine magnesium oxide showed intrinsic effects caused by the particle size on the surface basic properties (47). It was proposed that basic character depends more on domains and is enhanced in a large particle. The lower basic properties on the MgO/Al_2O_3 and $MgO–Al_2O_3$ prepared from hydrotalcite surfaces seems to be rationalized by smaller particle size of MgO.

Catalytic Actions of Alkali Ion-Exchanged Zeolites and Alkali Ion-Added Zeolites

The results listed in Table 5 indicate that alkali ion-exchanged zeolites exhibited low activities for the self-condensation of *n*-butyraldehyde. The low activities are explained by a relatively weak basicity of the alkali ion-exchanged zeolites as demonstrated in a previous study dealing with TPD of adsorbed CO_2 on alkali ion-exchanged and ion-added zeolites (19). The weakly basic property is considered to be due to the basic sites of the framework oxygen which has strongly covalent in nature (48, 49). Corma and co-workers have applied solid base catalysts to Knoevenagel condensation under mild conditions (50, 51). They reported that alkali ion-exchanged

zeolites exhibit a high selectivity for Knoevenagel condensation but cannot catalyze self-aldol condensation on ketonic group of a molecule containing activated methylene groups. They suggested that aldol condensation requires relatively strong basic sites, and, therefore, the reaction does not take place over alkali ion-exchanged zeolites with a weak basicity.

The formation of the trimeric glycol ester was obsrved for the alkali ion-exchanged zeolites. The ratios of the aldol condensation dimer to the trimeric glycol ester were higher for alkali ion-exchanged zeolites than for MgO and CaO, and lower than for alkali ion-modified alumina catalysts. In addition, the alkali ion-exchanged zeolites exhibited a high selectivity for 2-ethyl-2-hexenal. These results indicate that the acidic sites remain on the alkali ion-exchanged zeolites. Although a complete exchange of the protons by alkali ions is expected to result in neutralization of the acidic sites on zeolites, the existence of the acidic sites on the alkali ion-exchanged zeolites (52) and the important role of the acidic sites for base-catalyzed reactions were reported (53, 54). One might expect the high selectivity for *n*-butyl-*n*-butyrate produced by the Tishchenko-type self-esterification because the alkali ion-exchanged zeolites possess the acidic sites and the weakly basic sites. However, no conversion to *n*-butyl-*n*-butyrate for alkali ion-exchanged zeolites was observed in the present study.

High activities observed for the alkali ion-added zeolites are caused by the generation of strong basic sites on alkali ion-added zeolites (18, 19, 55). The formations of the trimeric glycol ester and 2-ethyl-2-hexenal were not suppressed for the alkali ion-added zeolites, which is in contrast to a complete suppression of the formation of the trimeric glycol ester observed for alkali ion-modified alumina catalysts. This shows that the modification with excess alkali ions improves the activity of zeolites not only for aldol condensation but also for Tishchenko-type cross-esterification. It is suggested that the modification with alkali ions is different for zeolite and for γ-Al_2O_3.

ACKNOWLEDGMENT

This work was supported by a Grant-in-Aid for Scientific Research, the Ministry of Education, Science and Culture, Japan.

REFERENCES

1. Hattori, H., *in* "Heterogeneous Catalysis and Fine Chemicals III" (M. Guisnet *et al.*, Eds.), p. 35. Elsevier, Amsterdam, 1993.
2. Malinowski, S., and Basinski, S., *Rocz. Chem.* **41,** 202 (1962).
3. Malinowski, S., and Basinski, S., *J. Catal.* **2,** 203 (1963).
4. Kiewlicz, S., and Malinowski, S., *Rocz. Chem.* **44,** 1895 (1970).
5. Malinowski, S., and Zielinski, B., *Bull. Acad. Pol. Sci., Ser. Sci. Chim.* **20,** 1015 (1972).
6. Reichle, W. T., *J. Catal.* **63,** 295 (1980).
7. Klaassen, A. W., and Hill, C. G., Jr., *J.Catal.* **69,** 299 (1981).
8. Ananthan, S., Venkatasubramanian, N., and Pillai, C. N., *J. Catal.* **89,** 489 (1984).
9. Reichle, W. T., *J. Catal.* **94,** 547 (1985).
10. Suzuki, E., and Ono, Y., *Bull. Chem. Soc. Jpn.* **61,** 1008 (1988).
11. Zhang, G., Hattori, H., and Tanabe, K., *Appl. Catal.* **36,** 189 (1988).
12. Zhang, G., Hattori, H., and Tanabe, K., *Appl. Catal.* **48,** 63 (1989).
13. Maltens, L. R., Vermeiren, W. J., Huybrechts, D. R., Grobet, P. J., and Jacobs, P. A., *in* "Proceedings, 9th International Congress on Catalysis, Calgary, 1988" (M. J. Phillips and M. Ternan, Eds.), Vol. 1, p. 420. Chem. Institute of Canada, Ottawa, 1988.
14. Swift, H. E., Bozik, J. E., and Massoth, F. E., *J. Catal.* **15,** 407 (1969).
15. Moggi, P., and Albanesi, G., *React. Kinet. Catal. Lett.* **22,** 247 (1983).
16. Nondek, L., and Malek, J., *Collect. Czech. Chem. Commun.* **44,** 2384 (1984).
17. Zhang, G., Hattori, H., and Tanabe, K., *Bull. Chem. Soc. Jpn.* **62,** 2070 (1989).
18. Hathaway, P. E., and Davis, M. E., *J. Catal.* **116,** 263 (1989).
19. Tsuji, H., Yagi, F., and Hattori, H., *Chem. Lett.*, 1881 (1991).
20. Miyata, S., Kumura, T., Hattori, H., and Tanabe, K., *Nippon Kagaku Zasshi* **92,** 514 (1971).
21. Villani, F. J., and Nord, F. F., *J. Am. Chem. Soc.* **69,** 2605 (1947).
22. Coluccia, S., Garrone, E., and Borello, E., *J. Chem. Soc., Faraday Trans. 1* **79,** 607 (1983).
23. Borello, E., Coluccia, S., and Garrone, E., *J. Catal.* **93,** 531 (1985).
24. Muzart, J., *Synthesis*, 60 (1982).
25. Zhang, G., Hattori, H., and Tanabe, K., *React. Kinet. Catal. Lett.* **34,** 255 (1987).
26. Texier-Boullet, F., and Foucaud, A., *Tetrahedron Lett.* **23,** 4927 (1982).
27. Rosini, G., and Marotta, E., *Synthesis*, 237 (1986).
28. Kordulis, C., Vordonis, L., Lycourghiotis, A., and Pomonis, P., *J. Chem. Soc., Faraday Trans. 1* **83,** 627 (1987).
29. Tanabe, K., and Saito, K., *J. Catal.* **35,** 247 (1974).
30. Kulpinski, M. S., and Nord, F. F., *Nature* **151,** 363 (1943).
31. Kulpinski, M. S., and Nord, F. F., *J. Org. Chem.* **8,** 256 (1943).
32. Yoshino, N., and Akutsu, H., *Nippon Kagaku Kaishi*, 742 (1978).
33. Zecchina, A., and Stone F. S., *J. Catal.* **101,** 227 (1986).
34. Coluccia, S., and Tench, A. J., *in* "Proceedings, 7th International Congress on Catalysis, Tokyo, 1980" (T. Seiyama and K. Tanabe, Eds.), Part B, p. 1154. Elsevier, Amsterdam, 1981.
35. Ito, T., Sekino, T., Moriai, N., and Tokuda, T., *J. Chem. Soc., Faraday Trans. 1* **77,** 2181 (1981).
36. Coluccia, S., Boccuzzi, F., Ghiotti, G., and Morterra, C., *J. Chem. Soc., Faraday Trans. 1* **78,** 2111 (1982).
37. Ito, T., Murakami, T., and Tokuda, T., *J. Chem. Soc., Faraday Trans. 1* **79,** 913 (1983).
38. Utiyama, M., Hattori, H., and Tanabe, K., *J.Catal.* **53,** 237 (1978).
39. Garrone, E., and Stone, F. S., *in* "Proceedings, 8th International Congress on Catalysis, Berlin, 1984," Vol. 3, p. 441. Dechema, Frankfurt-am-Main, 1984.
40. Hoq, M. F., Nieves, I., and Klabunde, K. J., *J. Catal.* **123,** 349 (1990).
41. Zecchina, A., Lofthouse, M. G., and Stone, F. S., *J. Chem. Soc., Faraday Trans. 1* **71,** 1476 (1975).
42. Satoko, C., Tsukada, M., and Adachi, H., *J. Phys. Soc. Jpn.* **45,** 1333 (1978).
43. Kawakami, H., and Yoshida, S., *J. Chem. Soc., Faraday Trans. 2* **80,** 921 (1984).
44. Yamaguchi, T., Morita, T., Salama, T. M., and Tanabe, K., *Catal. Lett.* **4,** 1 (1990).

45. Schaper, H., Berg-Slot, J. J., and Stork, W. H. J., *Appl. Catal.* **54,** 79 (1989).
46. McKenzie, A. L., Fishel, C. T., and Davis, R. J., *J. Catal.* **138,** 547 (1992).
47. Itoh, H., Utamapanya, S., Stark, J. V., Klabunde, K. J., and Schlup, J. R., *Chem. Mater.* **5,** 71 (1993).
48. Mortier, W. J., *J. Catal.* **55,** 138 (1978).
49. Okamoto, Y., Ogawa, M., Maezawa, A., and Imanaka, T., *J. Catal.* **112,** 427 (1988).
50. Corma, A., Fornés, V., Martín-Aranda, R. M., García, H., and Primo, J., *Appl. Catal.* **59,** 237 (1990).
51. Corma, A., and Martín-Aranda, R. M., *J. Catal.* **130,** 130 (1991).
52. Barthomeuf, D., *J. Phys. Chem.* **88,** 42 (1984).
53. Onaka, M., Kawai, M., and Izumi, Y., *Chem. Lett.*, 1101 (1983).
54. Itoh, H., Hattori, T., Suzuki, K., Miyamoto, A., and Murakami, Y., *J. Catal.* **72,** 170 (1981).
55. Laspéras, M., Cambon, H., Brunel, D., Rodriguez, I., and Geneste, P., *Microporous Mater.* **1,** 343 (1993).